



HAL
open science

Responses of wood formation to bending: a matter of dose and sensitivity adjustments

Jeanne Roignant, Éric Badel, Nathalie Leblanc-Fournier, Nicole Brunel-Michac, Julien Ruelle, Bruno Moulia, Mélanie Decourteix

► To cite this version:

Jeanne Roignant, Éric Badel, Nathalie Leblanc-Fournier, Nicole Brunel-Michac, Julien Ruelle, et al.. Responses of wood formation to bending: a matter of dose and sensitivity adjustments. *Trees - Structure and Function*, 2024, 38 (5), pp.1137-1150. 10.1007/s00468-024-02541-6 . hal-04846836

HAL Id: hal-04846836

<https://hal.science/hal-04846836v1>

Submitted on 18 Dec 2024

HAL is a multi-disciplinary open access archive for the deposit and dissemination of scientific research documents, whether they are published or not. The documents may come from teaching and research institutions in France or abroad, or from public or private research centers.

L'archive ouverte pluridisciplinaire **HAL**, est destinée au dépôt et à la diffusion de documents scientifiques de niveau recherche, publiés ou non, émanant des établissements d'enseignement et de recherche français ou étrangers, des laboratoires publics ou privés.



Distributed under a Creative Commons Attribution 4.0 International License

1 **ORIGINAL ARTICLE**

2
3 **Responses of wood formation to bending: a matter of dose and**
4 **sensitivity adjustments**

5
6
7 **Jeanne Roignant¹, Éric Badel¹, Nathalie Leblanc-Fournier¹, Nicole Brunel-Michac¹,**
8 **Julien Ruelle², Bruno Moulia¹ and Mélanie Decourteix^{1*}**

9 ¹Université Clermont Auvergne, INRAE, PIAF, F-63000 Clermont-Ferrand, France

10 ² Université de Lorraine, AgroParisTech, INRAE, UMR Silva, F-54000, Nancy, France

11
12 Running title: The impact of the dose of bending on wood formation.

13 *Author for correspondence: melanie.decourteix@uca.fr

14
15
16 **ACKNOWLEDGEMENTS**

17 We thank Christelle Boisselet, Patrice Chaleil, Aline Faure, Jérôme Franchel, Caroline Savel,
18 Brigitte Girard, Stéphane Ploquin for their technical help.

19 The authors would also like to thank SILVATECH (Silvatech, INRAE, 2018. Structural and
20 functional analysis of tree and wood Facility, doi: 10.15454/1.5572400113627854E12) from
21 UMR 1434 SILVA, 1136 IAM, 1138 BEF and 4370 EA LERMAB EEF research center INRAE
22 Nancy-Lorraine for the measurements of microfibril angle.

23
24
25
26

27 **Key message**

28 *In poplar stem, cell sensitivity to the dose of repeated bending drives wood formation toward*
29 *an egg-shaped cross section, thicker fiber cell walls and more fibers developing G- layers.*

30 **Abstract**

31 Trees acclimate to mechanical stimulations (*e.g.* wind) through thigmomorphogenesis. Recent
32 studies have demonstrated that repetitive unidirectional bending treatments applied to poplar
33 stems result in the production of two distinct types of wood: tensile flexure wood (TFW) on the
34 stretched side and compressive flexure wood (CFW) on the compressed side of the stem.
35 However, the dose-effect responses of wood formation to repeated unidirectional bending
36 treatments have not been established. In this study, we show that the number of bending events
37 plays a crucial role in wood formation.

38 To investigate this, young poplar stems were subjected to two different treatments involving
39 different numbers of transient and unidirectional elastic bends. The radial growth of the stems
40 was monitored throughout the treatments, and wood anatomy was quantitatively analyzed and
41 compared to control trees.

42 Observations revealed that the elliptic shape of poplar stem cross-section, observed in response
43 to the lowest dose, transformed into egg-shaped cross-section in response to the highest dose.
44 At the tissue level, cell differentiation and expansion were not differentially altered between
45 the two different treatments. However, there were notable differences in the proportion of G-
46 fibers and the thickening of secondary cell walls, showing that the different traits of flexure
47 wood have independent mechanosensitive control.

48 Overall, our findings demonstrate that, in addition to their ability to respond to the intensity and
49 direction of local mechanical strains, poplars adjust wood formation based on the number of
50 bending events. These modifications likely enhance stem resistance against breakage when
51 exposed to strong wind gusts.

52

53 **Keywords:** Poplar, mechanical stimuli, strain, dose-effect, mechanosensitivity, flexure wood,
54 bending, wood anatomy, secondary growth, cell wall, G-layer, thigmomorphogenesis

55

56 INTRODUCTION

57 The emergence of tissues providing a mechanical function was a key innovation for the
58 colonization of the terrestrial environment by land plants. While for aquatic plants water buoys
59 the plant body and offers mechanical support, land plants need to develop self-supporting aerial
60 structures. For trees, as they often grow tall, slender, and stiff stems, their mechanical stability
61 is constantly challenged by external mechanical loads, especially by wind-induced bending
62 stimulations (Gardiner et al. 2016). Trees sense and acclimate to such mechanical stimulations
63 by adjusting their growth and development, a process called thigmomorphogenesis (Jaffe
64 1973). Thigmomorphogenesis has been observed in many dicotyledonous species (herbaceous
65 and trees) and is usually characterized by a set of responses including a decrease in primary
66 growth, an increased secondary growth, and a higher development of root anchorage (Telewski
67 and Pruyn 1998; Coutand et al. 2008; Bonnesoeur et al. 2016). In nature, wind induces complex
68 and repeated back and forth bending stimuli in many directions and with many frequencies
69 (Gardiner et al. 2016; Bonnesoeur et al. 2016). Analysing this thigmomorphogenetic syndrome
70 mechanistically requires however simpler controlled and quantified bending stimulations.
71 Unidirectional bending stimulations of controlled intensity are a key to this analysis.
72 Biomechanical studies conducted on tomato and poplar demonstrated that the responses of
73 primary growth (in tomato) and of secondary growth (in poplar) to bending stimulations are
74 driven by the sensing of longitudinal mechanical strains. This relation has been formalized
75 through the ‘Sum of Strain Sensing’ (S^3m) integrative model (Coutand and Moulia 2000;
76 Coutand et al. 2009; Moulia et al. 2015). Beside such global effect on growth, it was observed
77 that secondary growth is more highly stimulated in the direction of maximal mechanical
78 stimulation. This was observed in response to bidirectional (back and forth) bending treatments
79 (Telewski and Jaffe 1981 in *Pinus Taeda*; Telewski 1989 in *Abies fraseri*; Pruyn et al. 2000 in
80 *Populus*). More recently, using unidirectional bending stimulations, Roignant et al. (2018) and

81 Niez et al. (2019) demonstrated, that in the bent portion of the stem of young poplars, the
82 secondary growth response is highly localized along the circumference of the cross-section of
83 the stem. Its intensity depends on the local intensity of the absolute value of longitudinal strains.
84 Indeed, the cross-section of poplar stem gets more elliptic as a result of an increased radial
85 growth along the radii that experiences the highest longitudinal strains during bending. By using
86 a finite element modelling approach, Niez et al. (2019) demonstrated that such allocation of
87 growth (and hence of wood biomass) along the bending direction increases both the stem
88 bending rigidity and its resistance to breakage (strength) compared to a circular cross-section
89 with the same construction cost. These results validated the hypothesis that, although costly for
90 the plants, thigmomorphogenesis is a crucial process for plants stability in a mechanically
91 fluctuating environment.

92 The mechanical properties of a structure, like its bending strength, depend not only on the sizes
93 of the structure, but also on the properties of the materials it is made of. Thus, mechanical
94 properties of plant stems may depend on both its geometry and its tissues composition. In
95 addition to changes in growth rates, changes in tissues composition are encountered in response
96 to environmental cues. But the relation between external mechanical stimuli and plant responses
97 at the tissue level has been overlooked in the literature. Regarding the effect of wind-related
98 bending stimulations, the main efforts have been put into the study of wood formation. In a few
99 genera such as *Abies* (Telewski 1989), *Pinus* (Telewski and Jaffe 1986) or *Populus* (Kern et al.
100 2005), multiple multidirectional bending treatments were shown to impact wood formation and
101 to conduct to the formation of a particular wood called “flexure wood” (Telewski 2016). To
102 investigate the mechanisms involved in the response of cambial and wood cells to stem bending,
103 unidirectional transient bending treatments of constant intensity were used (Roignant et al.
104 2018). In such experiments, a given cell is submitted to a maximal bending strain of constant
105 intensity and sign (*i.e.* only compressive or tensile strain) at each successive bending

106 stimulation. This has revealed that the wood formed under tensile flexural strains (Tensile
107 Flexure Wood; TFW) differs from a wood formed under compressive flexural strains
108 (Compressive Flexure Wood; CFW) (Roignant et al. 2018). Both share common anatomical
109 deviations from normal wood. For example, in both types of flexure wood (TFW and CFW)
110 vessel frequency is decreased, the diameter of wood fibres without a G-layer is increased and
111 their cell wall thickness is increased. However, other anatomical traits are differentially
112 modulated in Tensile and in Compressive Flexure Wood. Notably, the decrease in vessel
113 diameter or the formation of a tertiary cell wall layer with typical features of a G-layer (Clair
114 et al. 2018) in the fibres are specific to Tensile Flexure Wood (Roignant et al. 2018).

115 Altogether, it is now established that the absolute value of the intensity of the strains drives
116 radial growth while a combination of the intensity and the sign of strains pilots wood
117 differentiation in response to bending. Moreover, several studies suggest the importance of
118 taking the dose of stimulations during repeated stimuli into account. When considering a stem
119 bending treatment, the dose can be described as the product of three parameters: 1) the
120 frequency of recurrence of the stimulus, 2) the duration of the treatment (with frequency x
121 duration determining the total number of stimuli), and 3) the intensity of the stimulus. A dose-
122 response is thus an additive response to the sum of the intensity of each successive stimulus,
123 accumulated over time. In species having an herbaceous or bushy growth habit, the main corpus
124 of the studies on dose effects focused on responses to multiple unquantified stimuli such as
125 rubbing or brushing (especially stem elongation inhibition, changes in biomass production or
126 in flowering, Jaffe et al. 1980; Garner and Bjorkman 1996; Cipollini 1999, Morel et al. 2012),
127 indicating that repeating the bending stimuli has an effect but precluding further analysis. In
128 tree species, the consequences of multiple bending treatments on longitudinal and radial growth
129 were studied in more details. Using varied numbers of bending treatments per days, Telewski
130 and Pruyn (1998) compared the growth of the stems of non-staked *Ulmus americana* sapling to

131 the growth of staked or non-staked but manually bent stems. After 3 weeks of mechanical
132 treatment, height growth was reduced in “non-staked control” trees compared to “staked
133 control” trees and even more greatly reduced in trees manually flexed 5 to 80 times a day. Stem
134 diameter was increased in manually bent and “non-staked control” trees compared to “staked
135 control” trees. However, only the treatment made of 5 bending events per day significantly
136 increased radial growth (when compared to non-staked control trees); there was no further
137 additional secondary growth when the daily number of bending stimuli was further increased.
138 In this study, although the lateral displacement of the tip of the stem was controlled, the applied
139 strains were uncontrolled and unquantified. Indeed, as the applied strains strongly depend on
140 the diameter of the bent stem (Moullia et al. 2015), even if the stems were bent with the same
141 displacement of the stem tip all along the experiment, the intensities of strains were changing
142 along as secondary growth was increasing the stem diameter (in both a time- and bending
143 treatment-related ways). The study by Telewski and Pruyn (1998) thus revealed a complex
144 effect of the repetition of bending; but their experimental protocol precluded further analysis of
145 the dose-effect response. Later on, the effect of the dose was assessed by Coutand et al. (2009)
146 using controlled bending-strain stimuli. They first studied the effect of the intensity of a single
147 bending stimulus by varying the intensity of the strains. In this case, the responses of both i)
148 the radial growth, and (ii) the expression of *PtaZFP2*, a quantitative marker and major gene for
149 the molecular response to bending, were highly correlated to the sum of longitudinal strains
150 (integrated over the small portion of bent tissues) induced by the bending stimulus (Coutand et
151 al. 2009; Martin et al. 2014). They then applied recurrent daily bending and found that the first
152 three repeated bending events strongly increased radial growth compared to a single event,
153 suggesting an additive model of dose-response. However, after the third bending, the additive
154 effect was lost. These observations highlighted the existence of an accommodation process
155 (Martin et al. 2010; Leblanc-Fournier et al. 2014; Moullia et al. 2015). This lead Martin et al.

156 (2010) to propose an improved model (dose-accommodation model) in which the stem
157 desensitizes after a dose of 3 bending at 2% maximal strain. Such ‘accommodation’ is thought
158 to be crucial to avoid an over-response to recurrent stimulations like usual winds (Moullia et al.
159 2015; Bonnesoeur et al. 2016). However, this dose-accommodation model has never been
160 assessed for repeated stimuli of more than one bending per day.

161 Consequently, there is still a lack of knowledge about the dose-response effect of repetitive
162 bending on stem radial growth. This lack is even bigger when considering wood differentiation
163 responses. Indeed, the formation of Tensile and Compressive Flexure Wood was only studied
164 at the single frequency of 3 bending per week during 8 weeks (Roignant et al. 2018). We do
165 not know if conclusions from this study are still relevant in the case of different stimulation
166 regimes.

167 In this paper, we hypothesize that a higher number of bending stimulations may modify the
168 wood formation responses (*i.e.* circumferential distribution of radial growth and Flexure Wood
169 differentiation) previously observed in Roignant et al. (2018). We also make the hypothesis that
170 this response may be dose-dependent, but that the onset of an acclimative process may limit
171 this dependency to avoid non-acclimative over-responses. To test these hypotheses, we
172 complemented the results published in Roignant et al. (2018) for radial growth and wood
173 anatomy after 3 directional stimulations per week with results obtained after 15 stimulations
174 per week, for 8 weeks. We applied unidirectional bending stimulations of controlled intensity
175 which allowed us to assess heterogenous growth along the different radii of the cross-section
176 and to analyse both Compressive Flexure Wood and Tensile Flexure Wood.

177

178 **MATERIAL AND METHODS**

179 **Plant material and culture conditions**

180 Hybrid poplars (*Populus tremula* x *Populus alba*, clone INRA 717-1B4) were obtained by *in*
181 *vitro* micropropagation on MS ½ medium (Murashige and Skoog, 1962; Roignant et al. 2018).
182 After acclimation, young trees were transferred to a greenhouse at 22 (±1) °C (day) and
183 19 (±1) °C (night) with a relative air humidity of 60 ±10 %, under natural light. The trees were
184 planted in four-litre pots, in a substrate composed of one-third black peat and two-thirds local
185 clay-humic Limagne soil (Bornand et al. 1975). All trees were well watered throughout the
186 experiment. Five months after micropropagation, the poplars were ready for the experiments.
187 At that time, their stems had no branches and had a radius of about 6 mm at a height of 15 cm
188 above the ground. Their average length was 68 cm (comprised between 48 and 84cm). One
189 week before the first mechanical stimulations were applied, leaves were cut out from the basal
190 part of the stem (control trees included), on a 30 cm long portion. Data were collected from two
191 independent experiments (2015 and 2016), conducted during eight weeks at the same period of
192 the year (from May to July).

193 **Mechanical stimulations**

194 The choice of a range of frequencies of bending events was based on (1) the typical timing of
195 wind events in the natural habitat of the plant species, (2) our knowledge of the accommodation
196 capacities of poplar (Martin et al. 2010; Leblanc-Fournier et al. 2014). In a reference study of
197 the power spectrum of horizontal wind kinetic energy in temperate climates of the northern
198 hemisphere, Van der Hoven (1957) found 2 major eddy-energy peaks. The first one spans
199 mostly from periods of approximately 2 to 8 days, with a maximum at a mean period of 4 days.
200 It is related to the circulation of macro-meteorological cyclonic systems over the land. The
201 second one spans mostly from periods of 1 s to 10 min with a maximum at a period of 1 min.
202 It is related to the gusts of wind during a wind event. In between, there is a spectral gap from
203 periods of 10 min to 3 hours, for which there are almost no variation of wind kinetic energy due

204 to wind eddies. From this analysis, we chose to define two sets of important parameters
205 characterizing the artificial bending treatments:

206 (i) a number of days per week for which the trees are subjected to bending stimulations
207 (representing the alternation of windy and calm weather due to macro-
208 meteorological cyclonic events). For practical reasons, we retained two number of
209 days: 3 days of bending treatments followed by 4 days without any bending
210 treatment; that is 3 days of bending treatment per week, and 5 days of bending
211 treatment followed by 2 days with no stimulation, *i.e.* 5 days of bending treatments
212 a week. These two values frame the peak of period of macro-meteorological events,
213 while providing a simple organization of the experimental work.

214 (ii) the number of successive bending events in a row during one day (*i.e.* during a
215 simplified emulation of a micrometeorological storm event) and the time gap in
216 between. We retained 1 bending stimulation per day and 3 bending stimulations per
217 day. The maximal gap time in between successive bending was 3hours.

218 Thus, and to simplify the design, we only produced two extreme treatments noted 3-B/w and
219 15-B/w.

220 More precisely, the 3-B/w treatment consisted of a single unidirectional bend per day applied
221 at 9 am on the basal part of the stem (30 cm), for three consecutive days per week (Monday to
222 Wednesday,) followed by full rest during four days (Roignant et al. (2018); Fig.1a). This led to
223 a total amount of 3 bends per week (acronomized 3-B/w). The 15-B/w treatment consisted of
224 three unidirectional bending treatments per day (9am, noon, and 3 pm) for five consecutive
225 days per week (Monday, to Friday) and full rest during two days, leading to a total amount of
226 15 bends per week (hence the acronym 15-B/w). The two treatments were applied during eight
227 weeks.

228 Growth conditions were identical for the 3-B/w and the 15-B/w since both treatments were
229 carried out simultaneously, in the same greenhouse. The data for the low frequency treatment
230 called “3-B/w” were the one published in Roignant et al. (2018).

231 The intensity of the bending was controlled by a curved cylindrical plastic template providing
232 a spatially homogeneous curvature (Roignant et al. 2018; Fig.1). This geometrical configuration
233 provided a strain field which is homogeneous along the longitudinal direction, and that varies
234 linearly across the section of the stem (Coutand et al. 2009). Under these conditions, following
235 the diameter of the stem (parallel to the direction of bending) (Fig.1b), the longitudinal elastic
236 strains increase from zero at the so-called “neutral line”, up to the maximal strain intensity in
237 the outer cell layer. Above and below the neutral line, strains intensities are equal but of
238 different signs, as one part is submitted to tensile strains and the other to compressive ones.

239 For every tree and throughout the treatment period, we applied unidirectional transient bending
240 treatments (Fig.1a) with a maximum longitudinal strain of around 1 % (the maximal non-
241 injurious bending strain), and a duration of the loading-unloading cycle around 5 seconds. This
242 high value of strain was retained in an attempt to emulate more complex loading during high
243 but non-injurious wind events, that were shown to be important for thigmomorphogenesis
244 (Bonnesoeur et al. 2016). Trees were split up into three groups and submitted, or not, to
245 mechanical treatments: 12 trees were submitted to the 3-B/w treatment; 12 trees were submitted
246 to the 15-B/w treatment; 10 control trees grew without any mechanical stimulation. At the end
247 of the treatment, the bent segment of each stem was cut into several parts: we distinguished the
248 wood formed under tensile strains (stretched zone), under compressive strains (compressed
249 zone), and the area called “neutral zone”. The “neutral zone” surrounded the neutral line, which
250 theoretically experienced no strain (see Fig.1b and insert in the upper left corner Fig.4). Thus,
251 tissues in the neutral zone experienced very little strains.

252 **Growth analysis**

253 During the treatment period, the stem diameters were measured weekly with a digital calliper
254 in the direction of bending ($D_{//}$) and in the direction perpendicular to bending (D_{\perp}). $\Delta D_{//}$
255 corresponded to the growth in the direction where the applied longitudinal strain was the highest
256 (ε_{\max}), while ΔD_{\perp} corresponded to the neutral plane where the tissues experienced no
257 mechanical strain. The resulting ovalization of the stem cross-section was defined as in
258 Roignant et al. (2018):

$$259 \quad \text{Oval}(t) = \frac{D_{//}(t)}{D_{\perp}(t)} \quad (1)$$

260 where t is time (in weeks). We define ovalization as the process whereby the axi-symmetrical
261 round shape of the stem is changed to an oval shape; oval meaning a shape resembling either
262 an egg or an ellipse.

263 **Pith eccentricity**

264 The pith eccentricity, Ecc , represents the position of the pith along the diameter. The further
265 the pith from the geometrical centre, the higher the eccentricity (E). It was defined according
266 to Lenz's formula (Lenz 1954; Roignant et al. 2018) as:

$$267 \quad Ecc(\%) = \frac{e}{r} \times 100 \quad (2)$$

268 where e is distance between the geometrical centre of the pith and geometrical centre of the
269 stem cross-section, and r is the mean radius of the stem cross-section (computed with 60 rays).
270 Eccentricity was taken as positive if the geometric centre of the cross-section was on the side
271 where wood was stimulated under tension and negative if the geometric centre was located on
272 the side where wood was stimulated under compression.

273 **Histological analysis**

274 Histological analyses were realized as described in Roignant et al. (2018). Briefly, for vessel
275 diameter measurements, stem segments were embedded in polyethylene glycol (PEG;
276 molecular weight = 1500). Transverse sections (25 μm -thick) were cut with a microtome

277 (LEICA RM 2165 rotary, Jena, Germany) and stained with 1 % safranin–astra blue. For the
278 fibre cell wall measurements, small wood sticks were cut in the three sectors of interest, then
279 fixed, dehydrated, and infiltrated with medium-grade LR white resin as described in Azri et al.
280 (2009). Three to 4 µm thick sections were cut and stained with 0.5 % toluidine blue. Anatomical
281 traits were measured with ImageJ software (Schneider et al., 2012). The cell wall layers
282 thickness were measured on the samples embedded in LR white resin. Accurately,
283 distinguishing the primary wall layer with this technique remained difficult. Thus, we further
284 refer to cell wall layers (excluding G-layer) with the terminology “S layer”, merging the
285 primary and S1-S2 layers.

286 **Microfibril angle measurements**

287 The mean microfibril angles (MFA) of the cell wall layers were determined as described in
288 Roignant et al. (2018). Briefly, wood strips were sampled from debarked and oven-dried (48 h
289 at 104 °C) portions of bent and unbent stems. The MFA of crystalline cellulose was measured
290 at the SYLVATECH platform (INRAE, Nancy, France) with an X-ray diffractometer
291 (Supernova, Oxford-Diffraction, Abingdon-on-Thames, UK). The evaluation of mean MFA
292 was extracted from the 002 arc intensity curve using the method given in Verrill et al. (2006).

293 **Statistical analysis**

294 All measured and derived data were submitted to statistical analysis using R software (Team
295 R. Core 2014). The normal distributions of the data were tested by the Shapiro-Wilk test.
296 Analysis of variance (ANOVA) was used to determine whether anatomical parameters were
297 significantly different or not. In the case of significant differences between bent trees and
298 unbent trees, post-hoc analyses were based on the Tukey test.

299

300 **RESULTS**

301 ***The number of bending treatments modulates the secondary growth non-linearly***

302 The stem diameter in the direction parallel to the bending ($D_{//}$) was highly responsive to the
303 number of bending since it was x1.59 for 15-B/w and x1.38 for 3-B/w trees compared to control
304 trees at the end of the 8 week-long treatment (Table 1, Fig.2). This increase in final $D_{//}$ resulted
305 from an almost systematic higher weekly radial increment in 15-B/w trees compared to control
306 trees and 3-B/w trees (Fig.3). However, even though bending treatments were 5 times more
307 frequent in the 15-B/w than in the 3-B/w treatment, the response of the weekly radial increment
308 was only 1.55 higher (mean over the 8 weeks). Thus, the radial increment response of the stem
309 was non-linearly related to the frequency of the bending treatments.

310 *The number of stimulations enforces a breakage of the elliptical symmetry of the growth*
311 *response*

312 While the diameter perpendicular to the direction of bending (D_{\perp}) was not impacted by the 3-
313 B/w treatment, the 15-B/w trees presented a significantly higher D_{\perp} (7.2 mm for 15-B/w vs 6.5
314 mm for 3-B/w trees) (Table 1).

315 Both treatments increased the global ovalization of the stem. However, the ovalization of the
316 stem was not significantly modified between the two treatments (ovalization of 1.12 for the 3-
317 B/w trees and 1.14 for the 15-B/w trees). Contrary to the 3-B/w treatment, we observed a
318 significant negative pith eccentricity in response to the 15-B/w treatment, indicating that radial
319 growth increment was higher in the compressed zone. This particular circumferential
320 distribution of growth rate in 15-B/w trees leads to the formation of a stem with an egg-shaped
321 cross-section, instead of the elliptic cross-section observed in 3-B/w trees (Fig.2). To highlight
322 this shift toward the elliptic- and egg-shaped cross-section, we overlaid the actual shape of
323 the wooden region of typical cross-sections for each treatment (Fig.2) with elliptic (Fig.2e, 3-
324 B/w treatment) or ove-curve fits (egg shape) (Fig.2f, 15-B/w treatment) of these cross-sections.
325 The shape of the cross-section obtained with the 15-B/w treatment matches the ove-curve fit.
326 The shape of the cross-section obtained with the 3-B/w treatment matches the elliptic fit, except

327 on the sides of the compressed zone where the shape of the cross-section slightly departs from
328 the elliptic fit.

329 ***Bending strains greatly influence the growth and differentiation of wood cells, and this***
330 ***response is non-linear with the number of bending***

331 The effect of the two different bending treatments on wood cells differentiation was evaluated
332 by measuring several anatomical traits in the compressed, neutral, and stretched zones (Table
333 2, Fig.4). The 15-B/w treatment drastically decreased the vessel frequency by 28 % and 25 %
334 in the stretched and compressed zones respectively compared with control trees. However,
335 these values were not significantly different from the results obtained with the 3-B/w treatment
336 (-19 %). For both treatments, there was no effect of bending on vessel frequency in the neutral
337 zone. Vessel diameter was impacted in the stretched zone of bent stems only. The 3-B/w and
338 15-B/w treatments had similar effects, with vessel diameter being 8.2 % (3-B/w) and 7 % (15-
339 B/w) lower than in the control trees.

340 The proportion of fibres with a G-layer was responsive to the number of stretches. But this
341 increase in the G-fibre frequency responded non-linearly to the number of bending as this
342 proportion was only increased by x1.72 while quintupling the number of bending. As with the
343 3-B/w trees, the compressed and neutral zones of the 15-B/w trees were devoid of G-fibres.
344 Despite the higher number of fibres with a G-layer, the mean microfibril angle (MFA) was
345 similarly reduced in the stretched zone of both treatments.

346 In 3-B/w stems, the diameter of fibres without G-layer was slightly higher in the stretched and
347 compressed zones compared to fibres in the control trees. There was no significant difference
348 with the neutral zone of bent trees. Similar results were observed in the 15-B/w trees, except in
349 the compressed zone, where fibres diameter was higher compared to the neutral zone and the
350 control trees. The diameter of fibres with a G-layer, measured in the stretched zone, was 15 %
351 higher than in fibres of control trees for both the 3-B/w and the 15-B/w treatments.

352 ***Bending strains influence the thicknesses of the secondary cell-wall layers in wood fibres***

353 In 3-B/w trees, the mean S-layer thickness of fibres without G-layer (measured as the total of
354 the S1+S2+S3 cell wall layers) was 10 % thicker in the stretched and compressed zones
355 compared to control trees (Roignant et al. 2018). In the 15-B/w trees, it was thicker in the
356 stretched, neutral and compressed zones compared to the control. However, the cell wall
357 thickness in the compressed zone was significantly thicker (1.38 μm ; $p\text{-value}<0,05$) than in the
358 neutral (1.22 μm) and the stretched (1.26 μm) zones. Moreover, while the S-layer in the
359 stretched zone was identical between the two treatments, in the compressed zone of 15-B/w
360 trees, the S-layer significantly increased compared to the compressed zone of 3-B/w trees, but
361 only by 8%.

362 The S-layer of the G-fibres was identical between the 3-B/w and 15-B/w trees (0.79 μm and
363 0.77 μm respectively) in the stretched zone. However, the G-layer was significantly thicker in
364 15-B/w trees (1.54 μm) compared to 3-B/w trees (1.16 μm) by 19%.

365 **DISCUSSION**

366 ***The response of stem radial growth to the cumulated number of bending: more than***
367 ***longitudinal strain sensing!***

368 Previous experimental data obtained on angiosperm trees (Coutand et al. 2009; Moulia et al.
369 2015) showed that tree stem radial growth was impacted by the perception of the absolute value
370 of strains. More recently, Roignant et al. (2018) and Niez et al. (2019) showed that poplar stem
371 radial growth is influenced by the local intensity of these strains (in absolute value) at every
372 position around the cambium. As the absolute value of longitudinal strains is symmetrical
373 between the concave and convex sides of the cross section during pure bending, it was argued
374 that this could explain why the growth stimulations in the stretched and compressed part of the
375 stem were identical, leading to an elliptic shape.

376 In this study, in response to an increase of the number of bending stimulations from 3 per week
377 (3-B/w treatment) to 15 per week (15-B/w treatment), the radial growth kept being mostly
378 increased in the bending direction. However, the egg-shaped cross-section and the negative pith
379 eccentricity observed with the 15-B/w treatment showed that the stem radial growth response
380 to unilateral bending was asymmetric despite the symmetrical distribution of the absolute value
381 of the intensity of longitudinal strains. Thus, the absolute value of longitudinal strains is not
382 sufficient to explain the growth response.

383 Two candidate explanations can be given to explain the onset of an egg-shaped cross-section.
384 The first one is that, besides the number of longitudinal strains, radial elastic strains linked to
385 Poisson's ratio may also be influential. Basically, Poisson's ratio for elastic behaviour involves
386 a lateral shrinkage where the tissue is stretched longitudinally, and a lateral expansion where it
387 is compressed. In pure beam bending, this would mean lateral retraction in the zone under
388 longitudinal tensile strain and lateral expansion in the zone under longitudinal compressive
389 strain (see Fig 4a in Faroughi and Shaat (2018)). If we consider the cell scale, when the stem is
390 bent, the radial and tangential cell walls of cambial cells may then undergo Poisson's elastic
391 strains. In particular, in the zone that is longitudinally compressed, these walls are elastically
392 stretched in the radial and tangential directions. As cell wall expansion is known to be powered
393 by tensile stretching (Geitmann and Ortega 2009), Poisson stretching may enhance radial and
394 circumferential growth. However, assessing this hypothesis would require a detailed and
395 complex analysis of the elastic strain of the cross-section during bending. The second
396 explanation could be that radial growth is responsive to both the intensity and the sign of the
397 longitudinal strains, again to be challenged through a detailed biomechanical study. Whatever
398 the explanatory mechanism behind this behaviour, a question remains: How could one then
399 explain the elliptic shape (absence of egg shape) of the cross-section in the 3-B/w treatment?
400 Although an effect of the frequency of bending treatments on growth responses of the stem

401 cannot be ruled out, it is possible that the 3-B/w treatment also initiated an egg shape, without
402 us being able to identify it, for statistical reasons. Indeed, an incipient trend toward egg-shaping
403 seems likely from Fig.2e. Egg-shaping would thus be always present but its amount would
404 depend on the bending dose. To fully test this hypothesis, it would be interesting to verify if
405 applying the 3-B/w treatment for a longer period of time, or if applying the same regime with
406 a higher strain intensity, could lead to a clear egg-shaped cross-section too.

407 Using various numbers of bending treatments allowed to show that the growth and anatomical
408 response to bending treatments are more complex than initially suggested from the results based
409 on a smaller number of bending treatments. In particular, the local sensing of longitudinal strain
410 is not sufficient to account for the observed effect on radial growth. Modelling approaches
411 would be instrumental to decide between the above-stated new hypotheses about tree sensitive
412 capacities.

413 *The accommodation of growth responses to repeated loadings*

414 Bending stimulations induced by wind in natural conditions are characterized by varied
415 intensities, recurrences, and duration. It makes it difficult to distinguish the effects of these
416 three parameters. Here, we hypothesized the existence of a differential growth response to
417 different regimes of repeated stimuli. This response could possibly be of i) dose type (additive
418 response to the cumulated number of stimuli, that is to the product of the constant intensity to
419 the number of stimuli, or more generally the time integral of stimulus intensity over the duration
420 of the stimulus), or of ii) accommodation type involving changes in the mechanical sensitivity
421 along the repetitive loading (Martin et al. 2010) and hence a highly non-linear response.
422 Additionally, this response may even involve a specific frequency effect (that is an effect of
423 frequency for the same cumulated number of stimuli).

424 So far, very few studies described the response of tree radial growth to repetitive mechanical
425 stimulations and even fewer considered the loading dose. Telewski and Pruyn (1998) showed

426 that *Ulmus americana* stems (bent bidirectionally various times a day for three weeks) had the
427 same increase in radial growth when bent 5, 10, 20, 40 or 80 times a day, suggesting either
428 saturation or accommodation. Martin et al. (2010) investigated this aspect more accurately: they
429 submitted young poplars to a “7 Bending per week” (7-B/w) treatment during 1.3 week (*i.e.*
430 nine bending treatments with a 24 h lag time-interval) and compared their radial-growth
431 response with a computed theoretical model that assumed an additive effect of each bending
432 (dose model). They found that only the first three bending had an additive stimulatory effect.
433 Then the poplars were unable to respond to subsequent stimulations. This lead Martin et al.
434 (2010) to propose an improved dose-accommodation model in which the stem desensitizes after
435 a dose of 3 bending at 2% maximal strain. An even faster reduction in responsiveness was also
436 evidenced at the gene expression level (Martin et al. 2010; Pomiès et al. 2017): the vast majority
437 (96%) of genes that were differentially expressed after a first bending (at 2% max strain)
438 responded with lower level as soon as after the second bending that was applied 24 h after the
439 first stimulation (Pomiès et al. 2017). These growth and molecular phenomena provided the
440 first evidence of a tuning of the sensitivity to mechanical stimulations along stimulus history.
441 Such ‘accommodation’ is thought to avoid an over-response to recurrent stimulations like usual
442 winds (Moullia et al. 2015; Bonnesoeur et al. 2016).

443 In our experiments, the response of radial growth was not linearly related to the total number
444 of bending since radial growth was only 1.15 times higher (15-B/w *vs* 3-B/w) when trees were
445 treated with five times more bending. This falsifies a pure dose-response model and confirms
446 the ability of young poplar stems to accommodate the response of their secondary growth to
447 recurrent bending treatments with different bending regimes, as already observed by Martin et
448 al. (2010). Quantitatively though, the two experiments are not directly comparable: in Martin
449 et al. (2010), the strain intensity was 2%, and all the successive bending stimulations were
450 separated by a 24h lag time. In our experiments, the strain intensity was 1% and the repeated

451 bending protocol is longer and more complex, so that the 24h lag time only occurs in the 3-B/w
452 treatment. However, the dose-accommodation model (Martin et al 2010) makes this comparison
453 feasible. From their data, the desensitization was achieved for a strain dose of $3 \times 2\% = 6\%$. In
454 our experiments, the strain intensity was 1% so that a dose of 6% was achieved with 6 bending
455 stimulations. Since this dose is weekly exceeded with the 15-B/w treatment but not yet reached
456 with the 3-B/w treatment, the dose-accommodation model predicts that the 15-B/w treatment
457 would lead to a higher growth stimulation than the 3-B/w treatment, which matches our results.
458 Hence, our results do not falsify the dose-accommodation model. However, further mechanistic
459 investigations, reviewed in Leblanc-Fournier et al. (2014), have revealed that the
460 accommodation process at the molecular level starts up very early after a bending stimulation
461 and that the timing for its building up has to be taken into account (besides the simplistic idea
462 of a bending counting process). Therefore, additional experiments are now needed to fully
463 explore how bending amount and timing control stem sensitivity to bending.

464 Beyond accommodation to successive repeated bending stimulations, another important aspect
465 is the time to recover full sensitivity, so to characterize the entire desensitization-resensitization
466 cycle. In Martin et al. (2010), it took more than seven days for poplar stem to recover gradually
467 its full growth response capacity. In our experiments, desensitization-resensitization cycles
468 seemed to operate on shorter time scales (< one week) since radial growth of poplars responded
469 to each set of weekly bending stimulations without attenuation during the 8 weeks of treatment.

470 Thus, our results demonstrate for the first time that the dose of bending may influence the
471 kinetics of the desensitization-resensitization processes. Important research efforts are now
472 needed to specify more accurately this kinetics along the repeated stimuli and to concurrently
473 unravel the mechanisms underlying poplar stem sensitivity to bending.

474 ***Some, but not all, aspects of wood cells differentiation processes (enlargement and secondary***
475 ***wall formation) are sensitive to the number of repeated bending***

476 We first tested the hypothesis of a response of cell fate determination and cell expansion to
477 repeated bending. Histological analysis pointed out that the 15-B/w treatment affected vessel
478 frequency and vessel diameter similarly as the 3-B/w treatment, for both compressed and
479 stretched zones. Regarding fibres anatomy, we observed a similar increase in fibre diameter
480 both in the TFW and CFW of the 3-B/w and 15-B/w trees. This absence of an effect of the
481 number of bending stimuli on these three traits could be explained either by saturation of the
482 response or by the desensitization process, as already discussed for radial growth.

483 We then tested the hypothesis of an effect of the number of bending on cell wall thickening.
484 In fibres without G-layer, while the 3-B/w treatment promoted the formation of a thicker S-
485 layer (S1+S2) in both TFW and CFW, the 15-B/w treatment led to an even thicker S-layer for
486 the fibres in CFW. In fibres without G-layer, the response of the S-layer thickening to the
487 number of repeated strains thus seemed to depend on the sign of the strain.

488 Roignant et al. (2018) showed that about 18 % of wood fibres in the stretched zone of 3-B/w
489 trees presented the development of a G-layer. Here, we show that this proportion was highly
490 increased up to 31.9 % in response to the 15-B/w treatment. Thus, a higher number of bending
491 would conduct to a greater number of fibres activating the transcriptional program that is
492 necessary for G-layer formation. Moreover, in G-fibres of the 15-B/w trees, the G-layer was
493 thicker than in 3-B/w trees. Thus, G-layer initiation and formation seemed to respond to the
494 number of repeated bending. More frequent/numerous stimulations may activate the
495 transcriptional program that is necessary for G-layer formation in a higher number of fibres.

496 And exposing them to extra-stimulations would quantitatively stimulate this transcriptional
497 program or keep it active for a longer period of time, allowing the G-layer to get thicker.

498 Fang et al. (2007, 2008) observed a negative correlation between G-layer thickness and S-layer
499 thickness. In their conditions, when G-layer thickness increased, S-layer decreased. In our
500 study, the S-layer of G-fibres was decreased too in comparison to the S-layer of fibres in control

501 trees. However, even if the G-layer thickness was higher in the 15-B/w TFW, the S-layer
502 thickness of fibres developing a G-layer remained identical between the two treatments. We
503 propose the following qualitative model: (i) stem bending would trigger G-layer initiation; (ii)
504 this initiation would cancel S-layer development as suggested by Fang et al. (2007; 2008);
505 (iii) in the 15-B/w treatment, the time between two successive bending treatments would be
506 short enough for the process of G-layer deposit to be reactivated or prolonged in a single fiber
507 in response to a new bending stimulus thus conducting to an increased G-layer thickness.
508 The thickness of the G-layer being non-linearly related to the number of bending stimulations,
509 some but not all extra-bending in the 15-B/w treatment (compared to the 3-B/w treatment) may
510 reactivate or extend G-layer deposit. Thus, sensitivity adjustments may apply to G-layer
511 formation too.

512 ***Increasing the dose reveals new abilities of cells to respond to bending - an adaptive benefit?***

513 The mechanical properties of a tree stem depend on both its geometry and the intrinsic wood
514 properties. Considering two stems of different diameters made of a similar material, the thinner
515 one is more flexible than the thicker one with a dependency on the 4th power of the radius. The
516 higher increment of the diameter of 15-B/w stems compared to 3-B/w stems could be
517 considered as the very first steps of an adaptive advantage for trees: thanks to allometric
518 changes, the stem would become more rigid and more resistant to breakage when bent more
519 frequently, so when the risk of breakage increases. Moreover, we noticed that the very first
520 signs of a transition toward an egg shape can be observed at the end of the 3-B/w treatment,
521 while the final shape of the 15-B/w stems exhibited a clearer egg shape, characterized by a
522 wider section in the compression zone. Similar but more pronounced shape modifications have
523 been observed in poplar stems exposed to a 15-B/w bending treatment of similar strain intensity
524 (1%) over a x2.5 longer period of time (5 months instead of 8 weeks). In their theoretical
525 mechanical analysis, Niez et al. (2019) suggested that such an asymmetrical shape, with more

526 biomass allocated in the compression side, modifies the stress distribution in the transversal
527 cross-section and improves the mechanical safety of the stem. Given that ruptures occur more
528 easily when wood experiences compression than when it is stretched, Niez et al. (2019)
529 demonstrated that allocating biomass preferentially in the side under compression is a relevant
530 strategy for the mechanical resistance of the stem that constitutes an adaptive benefit when the
531 tree encounters external mechanical loadings. Our results show that for a similar duration,
532 increasing the number of bending hastens the ovalization of the stem toward the egg shape.
533 Thereby, increased repeated stimulations could accelerate the adaptative plastic response of the
534 tree.

535 In addition to geometry, the mechanical properties of the stem tissues, wood and bark,
536 contribute to the overall mechanical behaviour of a stem. For wood, longitudinal stiffness as
537 well as longitudinal strength is positively correlated with the basic density and negatively
538 correlated with microfibril angle (MFA) (Evans and Ilic 2001; Yang and Evans 2003; Niez et
539 al. 2020). The increase in the thickness of fibres cell walls in the zones experiencing maximal
540 strains (stretched or compressed), while keeping both the diameter of the fibres and the MFA
541 almost unchanged, suggests an improved mechanical stiffness and strength of these tissues
542 especially in the compressed zone of 15-B/w trees. The combination of the mechanical
543 reinforcement resulting both from the secondary growth (elliptical and egg shape reducing
544 bending stresses through their effect on the second moment of area) and wood differentiation
545 (increased cell wall thickness decreasing bending stress and increasing the resistance to cell-
546 wall buckling) may improve the weak point of the stem in compression during a bending event,
547 as recently suggested by Jacobsen et al. (2005) and Niez et al. (2019, 2020).

548

549 **CONCLUSION**

550 Trees can perceive mechanical strains, allowing them to adjust their shape and tissue
551 mechanical resistance to repetitive bending stimulations. In the case of unidirectional bending,
552 poplar trees produce special types of wood: Tensile Flexure Wood (TFW) on the stretched side,
553 and Compressive Flexure Wood (CFW) on the compressed side of the stem. Here we showed
554 that secondary growth responds to multiple stimulations according to the number of bending.
555 The control of every parameter of the dose stimulation allowed to disentangle the effect of strain
556 intensity from the number of stimulations. This highlighted that a high number of stimulations
557 leads to a non-linear response of secondary growth, especially in the region under compression.
558 It also emerged from anatomical analyses that processes related to cell wall formation, like G-
559 layer initiation and G-layer thickness in the TFW, are dose-sensitive whereas processes related
560 to cell fate determination and differentiation are not. Our results highlighted the complexity of
561 poplar stem responses to the dose of bending. They open new questions on the ability of trees
562 to adjust their sensitivity to mechanical loadings depending on their amount and recurrence. A
563 dynamic interplay between modelling and experimental approaches is now needed to progress
564 in our understanding of this accommodation phenomenon.

565

566

567

568 LITERATURE CITED

569 **Azri W, Chambon C, Herbette S, Brunel N, Coutand C, Leplé JC, Ben Rejeb I, Ammar S, Julien J-L,**
570 **Roeckel-Drevet P (2009)** Proteome analysis of apical and basal regions of poplar stems under gravitropic
571 stimulation. *Physiologia Plantarum* **136**: 193–208. DOI: 10.1111/j.1399-3054.2009.01230.x

572 **Bonnesoeur V, Constant T, Moulia B, Fournier M (2016)** Forest trees filter chronic wind-signals to acclimate
573 to high winds. *New Phytologist* **210**: 850–860. DOI: 10.1111/nph.13836

574 **Bornand M, Dejou J, Servant J (1975)** Les Terres noires de Limagne ; leurs différents faciès et leur place dans
575 la classification française des sols. *Comptes Rendus de l'Académie des Sciences Série D* **281** :1689-1692.

576 **Cipollini DF (1999)** Costs to Flowering of the Production of a Mechanically Hardened Phenotype in *Brassica*
577 *napus L.* *International Journal of Plant Sciences* **160**: 735-741. <https://doi.org/10.1086/314164>

578 **Clair B, Déjardin A, Pilate G, Alméras T (2018)** Is the G-Layer a Tertiary Cell Wall? *Frontiers in Plant*
579 *Science* **8**: 9-623. DOI: 10.3389/fpls.2018.00623

- 580 **Coutand C, Moulia B (2000)** Biomechanical study of the effect of a controlled bending on tomato stem
581 elongation: local strain sensing and spatial integration of the signal. *Journal of Experimental Botany* **51**:1825-42.
582 DOI: 10.1093/jexbot/51.352.1825
- 583 **Coutand C, Dupraz C, Jaouen G, Ploquin S, Adam B (2008)** Mechanical Stimuli Regulate the Allocation of
584 Biomass in Trees: Demonstration with Young *Prunus avium* Trees. *Annals of Botany* **101**: 1421–1432. DOI:
585 10.1093/aob/mcn054
- 586 **Coutand C, Martin L, Leblanc-Fournier N, Decourteix M, Julien J-L, Moulia B (2009)** Strain
587 Mechanosensing Quantitatively Controls Diameter Growth and PtaZFP2 Gene Expression in Poplar. *Plant*
588 *Physiology* **151**: 223–232. DOI: 10.1104/pp.109.138164
- 589 **Evans R, Ilic J (2001)** Rapid prediction of wood stiffness from microfibril angle and density. *Forest Products*
590 *Journal* **51**: 53-57.
- 591 **Fang CH, Clair B, Gril J, Alm eras T (2007)** Transverse shrinkage in G-fibers as a function of cell wall layering
592 and growth strain. *Wood Science and Technology* **41**: 659–671.
- 593 **Fang CH, Clair B, Gril J, Liu SQ (2008)** Growth stresses are highly controlled by the amount of G-layer in
594 poplar tension wood. *IAWA Journal* **29**: 237–246. <https://doi.org/10.1007/s00226-007-0148-3>
- 595 **Faroughi S and Shaat M (2018)** Poisson's ratio effects on the mechanics of auxetic nanobeams. *European Journal*
596 *of Mechanics – A/Solids* **70**: 8-14. <https://doi.org/10.1016/j.euromechsol.2018.01.011>
- 597 **Gardiner B, Berry P, Moulia B (2016)** Review: Wind impacts on plant growth, mechanics and damage. *Plant*
598 *Science* **245**: 94-118. <https://doi.org/10.1016/j.plantsci.2016.01.006>
- 599 **Garner LC, Bj orkman T (1996)** Mechanical conditioning for controlling excessive elongation in tomato
600 transplants: sensitivity to dose, frequency, and timing of brushing. *Journal of the American Society for*
601 *Horticultural Science* **121**: 894-900. DOI:10.21273/JASHS.121.5.894
- 602 **Geitmann A and Ortega JKE (2009)** Mechanics and modelling of plant cell growth. *Trends in Plant Science* **14**:
603 467-78. <https://doi.org/10.1016/j.tplants.2009.07.006>
- 604 **Jacobsen AL, Ewers FW, Pratt RB, Paddock WA, Davis SD (2005)** Do xylem fibers affect vessel cavitation
605 resistance? *Plant Physiology* **139**: 546–556. <https://doi.org/10.1104/pp.104.058404>
- 606 **Jaffe MJ (1973)** Thigmomorphogenesis: the response of plant growth and development to mechanical stimulation.
607 *Planta* **114**: 143–157. <https://doi.org/10.1007/BF00387472>
- 608 **Jaffe MJ (1980)** Morphogenetic responses of plants to mechanical stimuli or stress. *Bioscience* **30**:239-243.
609 <https://doi.org/10.2307/1307878>
- 610 **Jourez B, Avella-Shaw T (2003)** Effet de la dur ee d'application d'un stimulus gravitationnel sur la formation de
611 bois de tension et de bois oppos e dans de jeunes pousses de peuplier (*Populus euramericana cvGhoy*). *Annals of*
612 *forest science* **60**: 31–41. <https://doi.org/10.1051/forest:2002071>
- 613 **Kern KA, Ewers FW, Telewski FW, Koehler L (2005)** Mechanical perturbation affects conductivity,
614 mechanical properties and aboveground biomass of hybrid poplars. *Tree physiology* **25**: 1243–1251.
615 <https://doi.org/10.1093/treephys/25.10.1243>
- 616 **Leblanc-Fournier N, Martin L, Lenne C, Decourteix M (2014)** To respond or not to respond, the recurring
617 question in plant mechanosensitivity. *Frontiers in Plant Science* **5**: 401. <https://doi.org/10.3389/fpls.2014.00401>
- 618 **Lenz O. 1954.** *Le Bois de quelques peupliers de culture en Suisse*. ETH Zurich.
- 619 **Martin L, Leblanc-Fournier N, Julien J-L, Moulia B, Coutand C (2010)** Acclimation kinetics of physiological
620 and molecular responses of plants to multiple mechanical loadings. *Journal of Experimental Botany* **61**: 2403–
621 2412. <https://doi.org/10.1093/jxb/erq069>

- 622 **Martin L, Decourteix M, Badel E, Huguet S, Moulia B, Julien JL, Leblanc-Fournier N (2014)** The zinc finger
623 protein PtaZFP2 negatively controls stem growth and gene expression responsiveness to external mechanical loads
624 in poplar. *New Phytologist* **203**: 168-181. doi: 10.1111/nph.12781.
- 625 **Morel P, Crespel L, Galopin G, Moulia B (2012)** Effect of mechanical stimulation on the growth and branching
626 of garden rose. *Scientia Horticulturae* **135**: 59-64. <https://doi.org/10.1016/j.scienta.2011.12.007>
- 627 **Moulia B, Coutand C, Julien J-L (2015)** Mechanosensitive control of plant growth: bearing the load, sensing,
628 transducing, and responding. *Frontiers in Plant Science* **6**. <https://doi.org/10.3389/fpls.2015.00052>
- 629 **Murashige T, Skoog F (1962)** A Revised Medium for Rapid Growth and Bio Assays with Tobacco Tissue
630 Cultures. *Physiologia Plantarum* **15**: 473-497. <https://doi.org/10.1111/j.1399-3054.1962.tb08052.x>
- 631 **Niez B, Dlouha J, Moulia B, Badel E (2019)** Water-stressed or not, the mechanical acclimation is a priority
632 requirement for trees. *Trees* **33**: 279-291. <https://doi.org/10.1007/s00468-018-1776-y>
- 633 **Niez B, Dlouha J, Gril J, Ruelle J, Toussaint E, Moulia B, Badel E (2020)** Mechanical properties of “flexure
634 wood”: compressive stresses in living trees improve the mechanical resilience of Wood and its resistance to
635 damage. *Annals of forest science* **77**: 17. <https://doi.org/10.1007/s13595-020-0926-8>
- 636 **Pomiès L, Decourteix M, Franchel J, Moulia B, Leblanc-Fournier N (2017)** Poplar stem transcriptome is
637 massively remodelled in response to single or repeated mechanical stimuli. *BMC Genomics* **18**: 300.
638 <https://doi.org/10.1186/s12864-017-3670-1>
- 639 **Pruyn ML, Ewers BJ, and Telewski FW (2000)** Thigmomorphogenesis: changes in the morphology and
640 mechanical properties of two *Populus* hybrids in response to mechanical perturbation. *Tree Physiology* **20**: 535–
641 540. <https://doi.org/10.1093/treephys/20.8.535>
- 642 **Roignant J, Badel E, Leblanc-Fournier N, Brunel-Michac N, Ruelle J, Moulia B, Decourteix M (2018)**
643 Feeling stretched or compressed? The multiple mechanosensitive responses of wood formation to bending. *Annals*
644 *of botany* **121**: 1151-1161. <https://doi.org/10.1093/aob/mcx211>
- 645 **Schneider CA, Rasband WS, Eliceiri KW (2012)** NIH Image to ImageJ: 25 years of image analysis. *Nature*
646 *Methods* **9**: 671-675. <https://doi.org/10.1038/nmeth.2089>
- 647 **Team R. Core (2014)** *R: A language and environment for statistical computing*. R Foundation for Statistical
648 Computing, Vienna, Austria. 2013. ISBN 3-900051-07-0.
- 649 **Telewski FW (1989)** Structure and function of flexure wood in *Abies fraseri*. *Tree Physiology* **5**: 113–121.
650 <https://doi.org/10.1093/treephys/5.1.113>
- 651 **Telewski FW (2016)** Flexure Wood: Mechanical Stress Induced Secondary Xylem Formation. In: *Secondary*
652 *Xylem Biology*. Elsevier, 73–91. <https://doi.org/10.1016/B978-0-12-802185-9.00005-X>
- 653 **Telewski FW, Jaffe MJ (1981)** Thigmomorphogenesis: Changes in the morphology and chemical composition
654 induced by mechanical perturbation in six month old *Pinus taeda* seedlings. *Canadian Journal of Forest Research*
655 **11**:380-387. <https://doi.org/10.1139/x81-051>
- 656 **Telewski FW, Jaffe MJ (1986)** Thigmomorphogenesis: anatomical, morphological and mechanical analysis of
657 genetically different sibs of *Pinus taeda* in response to mechanical perturbation. *Physiologia Plantarum* **66**: 219–
658 226. <https://doi.org/10.1111/j.1399-3054.1986.tb02412.x>
- 659 **Telewski FW, Pruyn ML (1998)** Thigmomorphogenesis: a dose response to flexing in *Ulmus americana*
660 seedlings. *Tree physiology* **18**: 65–68. <https://doi.org/10.1093/treephys/18.1.65>
- 661 **Yang JL, Evans R (2003)** Prediction of MOE of eucalypt wood from microfibril angle and density. *Holz als Roh-*
662 *und Werkstoff* **61**: 449-452. <https://doi.org/10.1007/s00107-003-0424-3>

663 **STATEMENTS AND DECLARATIONS**

664 **Funding**

665 This work was supported by grants from the Auvergne Regional Council (“Programme
666 Nouveau Chercheur de la Région Auvergne-2014”) and from CNES (Centre National d’Etudes
667 Spatiales).

668 SILVATECH facility is supported by the French National Research Agency through the
669 Laboratory of Excellence ARBRE (ANR-11-LABX-0002-01).

670

671 **Competing interests**

672 The authors have no relevant financial or non-financial interests to disclose.

673

674 **Author contributions**

675 JR¹, MD and EB contributed to the study conception and design.

676 JR² performed the MFA measurements with the technical help of JR¹.

677 JR¹ and NBM performed all the other experiments. Data analysis was performed by JR¹.

678 The first draft of the manuscript was written by JR¹ and MD.

679 All the authors contributed to the writing of the final version of the manuscript.

680

681 **Data availability**

682 The datasets generated during and/or analysed during the current study are available from the
683 corresponding author on reasonable request.

684

685 **FIGURES LEGENDS**

686 **Fig.1** Schematic representation of a bending treatment.

687 (a) The leaves were removed on the basal part of the stem, on a 30cm long portion. Then, the
688 stem was unidirectionally bent on a template (portion of circle in dark grey). “Unidirectional
689 bending treatment/stimulation” means (1) displacement from the upright position to one side
690 against the template (duration is less than 3s), followed by (2) a return to the original upright
691 position (duration is less than 3s).

692 (b) The constant curvature of the template (quarter circle in dark grey) allows to impose a
693 pure bending to the stem. For clarity purposes, the curvature of the template is much higher
694 on the scheme than what was applied in the experiment.

695 ρ is the radius of the curved pattern; r is the radius of the stem. The blue arrows represent the
696 distribution of the intensities of longitudinal strains (either negative in the compressed zone,
697 or positive in the stretched zone) along the diameter parallel to the bending direction.

698 Maximal strain occurs at the periphery and its absolute value is equal to $\varepsilon = r/(r + \rho)$. ε_{\max} is
699 the maximal strain applied to the stem (at the periphery of the stem, in the direction parallel to
700 the bending direction).

701 L_0 is the initial length of the bent segment (30cm).

702 The ‘neutral line’ (dotted line in light grey) is a virtual line where longitudinal strain equals
703 zero.

704 **Fig.2** Repeated unidirectional bending treatments result in an egg-shaped stem cross-section.

705 Cross-section of *P. tremula* × *P. alba* without mechanical stimulation (a), after 8 weeks of 3-
706 B/w bending treatment (b) and after 8 weeks of 15-B/w bending treatment (c). Staining: 1 %
707 safranin–astra blue. The black arrow shows the direction of bending and red arrows show the
708 position of the cambium at the beginning of the mechanical treatments.

709 (d), (e), (f) the shape of the section of the wooden region in bent stems is compared to the shape
710 in control trees and to known geometrical shapes.

711 (d) (yellow dashed-line) manual circumferential outline of the wooden region and of the
712 anatomical centers of the cross-section of a control tree.

713 (e) the circumferential outline of a control tree (yellow dashed-line) is superimposed with the
714 circumferential outline (brown squared dashed-line) of 3-B/w trees and with an elliptic fit of
715 the cross-section (...)

716 (f) the circumferential outline of a control tree (yellow dashed-line) is superimposed with the
717 circumferential outline (orange dashed-line) of 15-B/w trees and with an ove-curve fit of the
718 cross-section (-.-)

719 ... elliptic fit of the cross-section in (B) (equation $\left(\frac{x}{a}\right)^2 + \left(\frac{y}{b}\right)^2 = c^2$)

720 -.- (egg-shaped) ove-curve fit of cross-section in (C) (equation $\left(\frac{x}{a}\right)^2 + \left(\frac{y}{(b+\beta x)}\right)^2 = c^2$)

721 Scale bar = 2 mm.

722 Data obtained with the 3-B/w treatment were published in Roignant et al. (2018).

723

724 **Fig.3** Effect of the weekly frequency of bending on secondary growth.

725 Cumulative radial increment of the stem of young poplar trees in response to different weekly
726 frequencies of bending, in 2015 and 2016 ((a) and (b) respectively).

727 Weekly radial increment of the stem of young poplar trees in response to different weekly
728 frequencies of bending, in 2015 and 2016 ((c) and (d) respectively).

729 Dotted lines refer to unbent (Ct) trees. Black triangles and grey squares refer to stems bent 3
730 times or 15 times a week respectively. Vertical bars represent standard errors.

731

732 **Fig.4** Impact of the weekly frequency of bending on several wood anatomical traits.

733 Anatomy details of *P. tremula* × *P. alba* without mechanical stimulation (a), after 8 weeks of
734 3-B/w bending treatment (b–d) and 15-B/w bending treatment (e – g). (b, e) Stretched zone; (c,
735 f) Neutral zone; (d, g) Compressed zone. (a1–g1; b2 and e2) Details of the cell wall fibres in
736 wood of (a) a control tree. (b1, b2, e1, e2) The stretched zone with (b1, e1) or without (b2, e2)
737 a G-layer; (c1, f1) the neutral zone; (d1, g1) the compressed zone. (a–g) samples were collected
738 and embedded in PEG, then cross-sections were stained with 1 % safranin–astra blue. (a1–g1;
739 b2 and e2) samples were collected and embedded in LR white resin, then stained with toluidine
740 blue.

741 Table 1: Morphological dimensions of stems after 8 weeks of mechanical stimulations with the
 742 3-B/w treatment (1 bending per day, 3 days per week) and the 15-B/w treatments (3 bending
 743 treatments per day, 5 days per week).

744 Means were obtained from the data of two independent experiments. Means (\pm s.e.) within each
 745 column with different letters are significantly different at $P < 0.05$ (ANOVA with a Tukey post-
 746 hoc test). $\Delta D_{//}$ and ΔD_{\perp} are the total diameter increases in the direction parallel and
 747 perpendicular to the bending respectively. Ovalization and pith eccentricity are computed
 748 according to equations (1) and equation (2) respectively. In this table, ovalization is computed
 749 by dividing the diameter parallel to the bending direction by the diameter perpendicular to the
 750 bending direction (values measured after 8 weeks of mechanical stimulations). Data obtained
 751 with the 3-B/w treatment were published in Roignant et al. (2018).

Morphological properties	Control	3-B/w	15-B/w
$\Delta D_{//}$ (mm)	5.8 ± 0.2^a	8.0 ± 0.2^b	9.2 ± 0.2^c
ΔD_{\perp} (mm)	5.8 ± 0.2^a	6.5 ± 0.2^a	7.2 ± 0.2^b
Ovalization ($D_{//}/D_{\perp}$)	1.01 ± 0.01^a	1.12 ± 0.01^b	1.14 ± 0.01^b
Pith eccentricity (%)	-0.4 ± 2.4^a	-4.8 ± 0.8^a	-6.4 ± 0.9^b

752

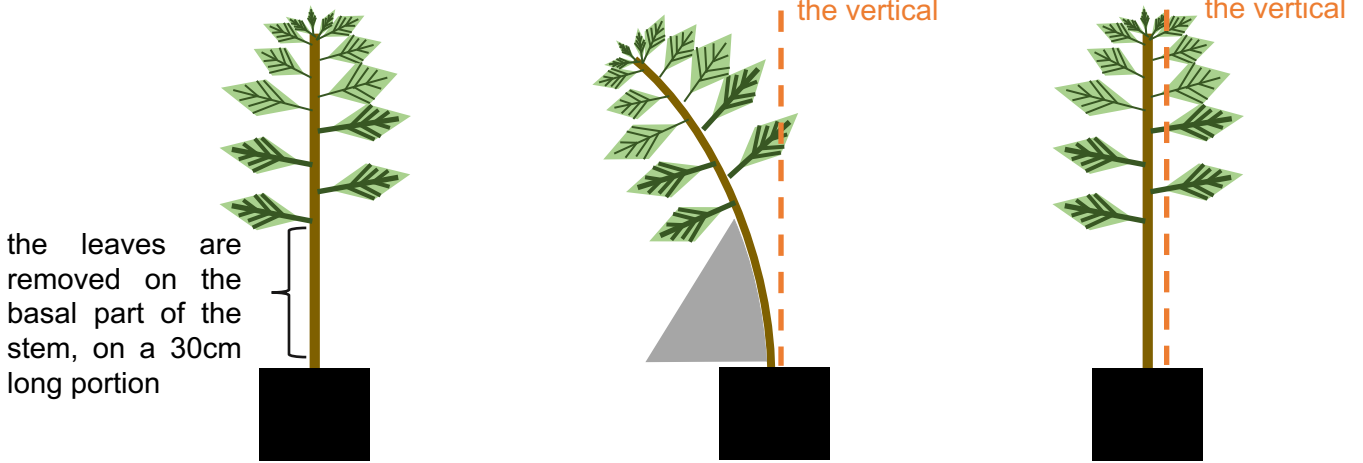
753 Table 2: Modifications of anatomical traits of wood in different zones of bent poplar stems (stretched, neutral and compressed zones) in response
 754 to the 3-B/w and 15-B/w treatments.
 755 (G) refers to fibres with a G-layer. Means (\pm s.e.) within each column with different letters are significantly different at $P < 0.05$ (ANOVA with a
 756 Tukey post-hoc test). Data obtained with the 3-B/w treatment were published in Roignant et al. (2018).

Anatomical properties	Stretched zone		Neutral zone		Compressed zone		
	Control	3-B/w	15-B/w	3-B/w	15-B/w	3-B/w	15-B/w
Vessel frequency (No. /mm ²)	187 ^a	151 ^{bc}	134 ^c	176 ^a	162 ^{ab}	151 ^{bc}	140 ^c
Vessel diameter (μ m)	38 \pm 0.7 ^a	34 \pm 0.6 ^b	35 \pm 0.6 ^b	37 \pm 0.5 ^a	39 \pm 0.3 ^a	37 \pm 0.6 ^a	38 \pm 0.7 ^a
Fibre diameter (μ m)	13.9 \pm 0.4 ^a	14.8 \pm 0.4 ^{bc} 16 \pm 0.3 (G) ^d	14.9 \pm 0.3 ^{bc} 16,3 \pm 0.5 (G) ^d	14.1 \pm 0.3 ^{ab}	14.5 \pm 0.3 ^{ab}	14.9 \pm 0.4 ^{bc}	15.4 \pm 0.3 ^{cd}
G-fibre proportion (%)	1.9 \pm 0.5 ^a	18.6 \pm 1.8 ^c	31.9 \pm 2.5 ^d	0.7 \pm 0.1 ^b	0.9 \pm 0.2 ^b	0.6 \pm 0.1 ^b	0.6 \pm 0.2 ^b
S-layer thickness (μ m)	1.1 \pm 0.03 ^a	1.3 \pm 0.05 ^{cd} 0.79 \pm 0.03 (G) ^f	1.3 \pm 0.03 ^d 0.77 \pm 0.04 (G) ^f	1.2 \pm 0.02 ^{ab}	1.2 \pm 0.05 ^{bc}	1.3 \pm 0.06 ^{cd}	1.4 \pm 0.03 ^e
G-layer thickness (μ m)	-	1.16 \pm 0.05 ^a	1.54 \pm 0.8 ^b	-	-	-	-
Microfibril angle (MFA) ($^{\circ}$)	28 ^a	23 ^b	22 ^b	27 ^a	27 ^a	27 ^a	28 ^a

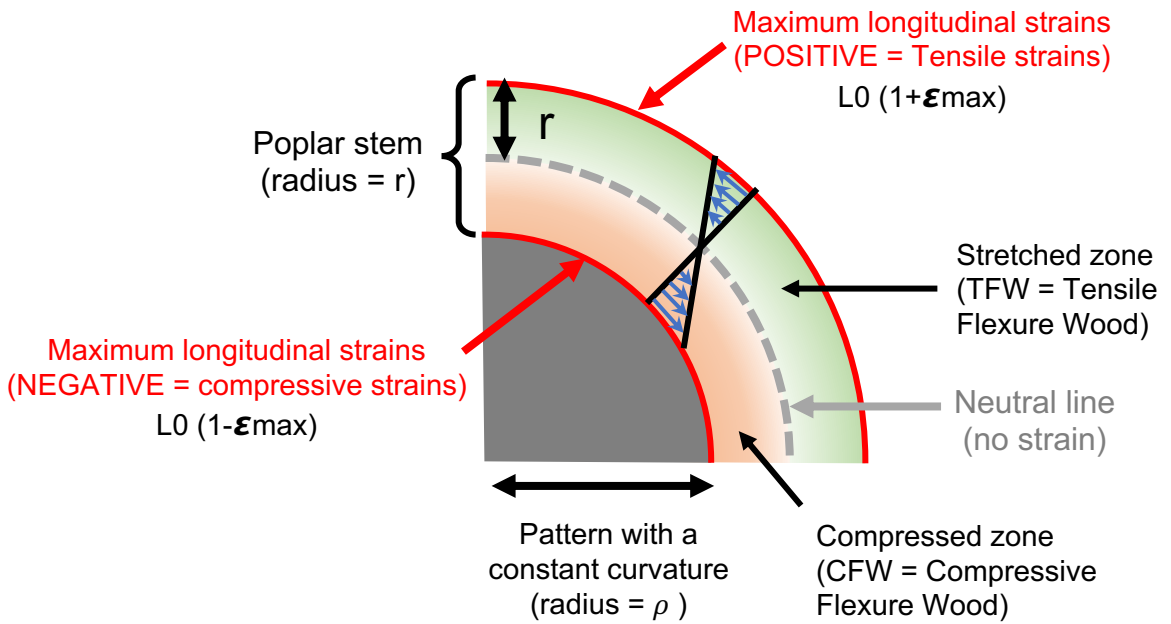
757

Fig 1

(a)



(b)



Longitudinal plane

Fig 2

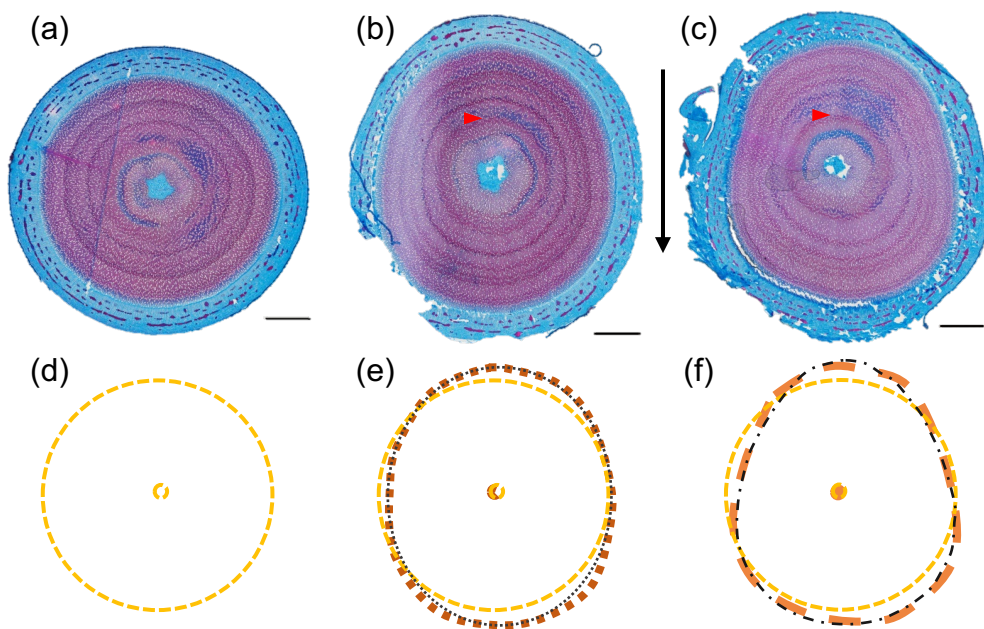


FIG3

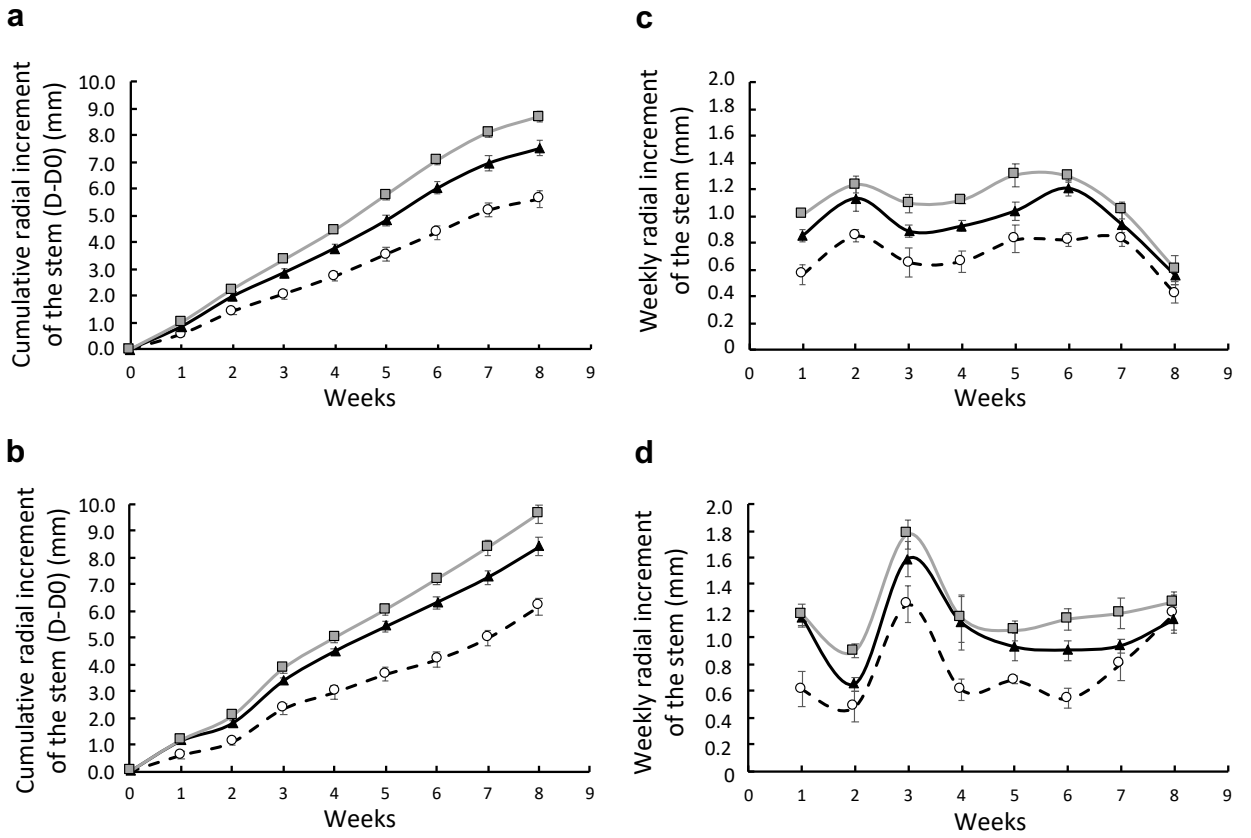


FIG4

